A Novel Integrated Hydrothermal Liquefaction and Solar Catalytic Reforming Method for Enhanced Hydrogen Generation from Biomass

Anuradha Shende, Richa Tungal, Rajneesh Jaswal, Rajesh Shende[*]

Department of Chemical and Biological Engineering, South Dakota School of Mines & Technology, Rapid City, South Dakota, USA
*Corresponding author: rajesh.shende@sdsmt.edu

Abstract Short energy intensive hydrothermal liquefaction (HTL) of biomass in the presence of Ni salt catalyst selectively generates H_2 in the product gas and biocrude mainly containing C_1-C_3 acids (formic, lactic, propionic, acetic), HMF and furfural. The H_2 mass balance indicated that only 3.12 vol% H_2 in biomass (cotton) was released as product gas; 48.7 vol% was captured in the C_1-C_3 acids while the remainder H_2 was trapped in oxygenated compounds and char. Continuing HTL after 120 minutes caused no further increase in gas phase H_2 yields. To enhance the H_2 yields with minimal energy input, solar photocatalytic reforming (PR) of the biocrude with Pt/TiO_2 catalyst was investigated. Photocatalysis of activated carbon (AC) treated biocrude generated an additional H_2, 17.82 wt%. H_2 yields from photoreforming of simulated biocrude acid mixture and actual biocrude were compared. Enhanced H_2 generation was observed with integrated HTL-PR of biomass.

Keywords: hydrogen, hydrothermal liquefaction, cotton, photoreforming, biocrude

Cite This Article: Anuradha Shende, Richa Tungal, Rajneesh Jaswal, and Rajesh Shende, "A Novel Integrated Hydrothermal Liquefaction and Solar Catalytic Reforming Method for Enhanced Hydrogen Generation from Biomass." *American Journal of Energy Research*, vol. 3, no. 1 (2015): 1-7. doi: 10.12691/ajer-3-1-1.

1. Introduction

World's current energy demand is primarily fulfilled by the use of fossil fuels, however, very little fraction of energy is derived from renewable resources [1]. Biomass is a renewable source of environmentally friendly high energy density (142 MJ/kg) hydrogen (H_2) fuel. In industry, majority of H_2 is produced by steam reforming of non-renewable resources such as the natural gas and petroleum. With rapid depletion of these resources, many researchers are exploring biological [2], pyrolysis [3], gasification [4], hydrothermal liquefaction (HTL) [5,6] and photoreforming [7,8] processes for H_2 generation from renewable biomass, biomass waste and biomass components. However, each of these technologies suffer from drawbacks ranging from high energy input to low conversion efficiencies pointing to a need to develop energy efficient viable routes for H_2 generation from renewable sources.

Hydrothermal liquefaction (HTL) under subcritical conditions transforms a biomass into gaseous products, liquid biocrude and solid biochar. The composition of the biocrude and product gas is largely influenced by catalyst. In our previous work [9] on HTL of cellulose, xylan, lignin, wastepaper and pinewood, homogeneous Ni salt catalysts were found effective in generating H_2. HTL of pinewood at 275°C with $Ni(NO_3)2$ yielded 12.26 mol% H_2 [6]. Under similar experimental conditions, the authors

reported HTL of wastepaper resulted in 51% liquefaction with 10.2 mol % H_2 generation [5]. These HTL studies revealed longer processing time that resulted only in slight increase in H_2 yield with bicrude mainly forming CO_2 in the product gas. Biocrude typically contains intermediates such as saccharides, anhydrosugars, HMF, furfural, ketones, alcohols, carboxylic acids, lignin derived compounds [5]. Our studies with pinewood and waste paper have shown that the Ni salt catalyst promotes higher quantities of C_1-C_3 carboxylic acids in the biocrude. Several C_1-C_3 acids have been shown to be excellent sacrificial agents in photocatalyis for H_2 generation. There are many reports on photocatalysis of single acids for H_2 production. For e.g. photoreforming of lactic, acetic, benzoic, formic and oxalic acids has been investigated with the aim of simultaneous H_2 production and remediation of acidic wastewater [10,11,12]. However, H_2 yields from few real multi-component aqueous systems have been studied [13,14]. Photoreforming of wastewater systems containing multiple electron donors showed that the H_2 yields depend on several factors such as TiO_2 surface adsorption, chemical structure, concentration and the ratio of the electron donors [10]. To the best of our knowledge, photocatalysis of the complex multi-component biocrude for H_2 production is not yet reported.

In addition to acids and sugars, HTL derived biocrude contains several other compounds that may either contribute to the H_2 yield or may negatively affect photoreforming process. Lignin, tannin, and sugars interfering in downstream processes such as the microbial

fermentation have been removed using activated charcoal (AC) [15,16]. AC has also been used to remove toxic components from biocrude obtained from HTL of starch for downstream microbial processing [17]. Therefore, in this investigation, cotton biocrude was treated with AC to remove potential interfering compounds. Both, untreated and AC-treated biocrude were tested with PR process for the H_2 generation.

Chemically inert and inexpensive TiO_2 catalyst [18] was chosen for PR of biocrude. The band gap energy (E_g) of TiO_2 permits excitation of TiO_2 only by the UV-portion of the solar spectrum. Efforts can be found in the literature on modifying TiO_2 with suitable dopants to achieve visible light activation. Very recently, we reported TiO_2 modified ZnO/TiO_2 photocatalysts [19] with lower E_g that yielded higher H_2 volume from aqueous methanol.
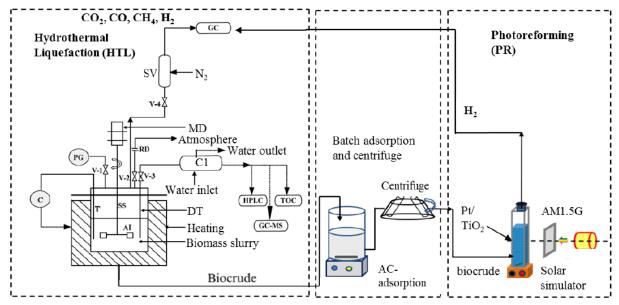

Figure 1. Schematic of integrated hydrothermal liquefaction (HTL) and photoreforming (PR) process for H_2 generation (GC: gas chromatography, GC-MS: gas chromatography-mass spectrometry, HPLC: high pressure liquid chromatography, TOC: total organic carbon, MD: magnetic drive, RD: rupture disk, SS: stainless steel, C: cooling water, C1: condenser, PG: pressure regulator, V1/V2/V3/V4: control needle valves, T: thermocouple, W: vessel SS304 mounted for gas sampling, AI: impeller)

Additionally, the rapid recombination of the photogenerated electrons with the holes limits H_2 production. Using co-catalyst such as platinum on TiO_2 surface traps photogenerated electrons and partially prevents electron-hole recombination [20]. The PR of biomass model compounds, such as the primary, secondary and tertiary alcohols, glycerol, sugars and a few carboxylic acids have been studied for H_2 generation [21]. It is expected that H_2 and CO_2 production from biocrude components will follow the general reforming scheme:

$$C_xH_yO_z + (2x\text{-}z)H_2O \xrightarrow{hv} xCO_2 + (2x\text{-}z+y/2)H_2 \quad (1)$$

Green solar photoreforming of the biocrude to H_2 will not only remediate the biocrude but also permit significantly higher H_2 abstraction from the biomass. In this study, HTL of cellulosic biomass was carried out at 250°C in the presence of $NiSO_4$ catalyst for the production of H_2 and biocrude containing C_1-C_3 carboxylic acids. The biocrude and its carboxylic acids were individually photoreformed to demonstrate additional yields of H_2. A schematic describing the combined HTL and PR process is shown in Figure 1. The results show that integrated HTL and PR process has a potential to develop into technologically feasible route for enhanced H_2 production.

2. Materials and Methods

2.1. Materials

Commercially available cotton balls (98% cellulose) were selected as biomass feedstock. Nickel sulphate

hexahydrate and dihydrogen hexachloroplatinate (IV) hydrate, Premion (99.999% metal basis) were purchased from Alfa Aesar, MA. Titanium (IV) oxide (P25 nanoparticles), 99.7% anatase (particle size ~ 25 nm, surface area 45-55 m^2/gm) was obtained from Sigma Aldrich. Filtrasorb 600 activated charcoal (Iodine number 850 mg/g) was purchased from Calgon Carbon.

2.1.1. Elemental Composition of Biomass

Biomass, cotton (1 gram) was dried at 45°C overnight in the oven and weighed the next day to determine moisture content. The moisture free cotton was supplied to the Midcontinent Testing Labs, Inc., Rapid City, SD, USA for the elemental analysis.

2.1.2. Preparation of Platinum Coated TiO_2 Nanoparticles

Platinum coating on TiO_2 nanoparticles was achieved by the wet incipient method. TiO_2 nanoparticles (0.5 g) were placed in water (12 ml) and sonicated for 30 min. To this dispersion, hexachloroplatinic acid (1 wt% Pt equivalent) was added and sonication was continued for additional 3 hrs. The dispersion was dried at 100°C and calcined at 600°C for 1 hrs. The platinum loading was determined by EDX analysis using Zeiss Supra 40VP scanning electron microscope/energy dispersive X-ray spectrometer.

2.1.3. Hydrothermal Liquefaction (HTL) of Biomass

A 300 ml high-temperature, high-pressure (HTHP) stainless steel (SS316) reactor (PARR Instrument Co,

Illinois) fitted with gas inlet, outlet valves, a liquid sampling valve, pressure gauge, rupture disc, magnetic drive and a thermocouple was used for HTL of biomass. Slurry of 1.0 gram cotton balls cut into 0.5 cm^2 pieces was made in 150 ml of distilled water containing 5 wt% $NiSO_4$ catalyst. The slurry was loaded in the reactor and stirred by an impeller at a constant speed of 1300 rpm. The reactor was pressurized to 40 psi with N_2 at room temperature and heated to 250°C to perform HTL for 120 min. During the HTL processing, gas and liquid samples were withdrawn periodically and analyzed by GC, HPLC and GC-MS. The processed slurry was centrifuged at 13000 rpm for 20 min to recover supernatant biocrude.

2.1.4. Characterization of Product Gas from HTHP Reactor Headspace

While HTL of biomass was in progress, product gas samples were withdrawn from the HTHP reactor headspace and analyzed on the Agilent7890A gas chromatograph (GC) equipped with thermal conductivity detector (TCD) and Porapak-Q stainless steel packed column (6 ft x 0.25 in x 2.1 mm) from Supelco. The GC oven was operated at 40°C and N_2 at 1 ml/min was used as a carrier gas. He (99.99% purity) was used to characterize gaseous carbon species. Calibration curves were prepared using specific gas standards purchased from the Matheson Gases, SD, USA and the product gas volumes were determined at the NTP (20°C and 1 atm) conditions.

2.1.5. Activated Carbon (AC) Treatment of Biocrude and Characterization of AC-treated Biocrude

To the biocrude obtained from HTL, activated carbon was added at two different concentrations of 10 mg/ml and 50 mg/ml. The mixture was left on a stirrer for 12 hours after which it was centrifuged. The clear supernatant was kept at 4°C until ready to use. The biocrude was analyzed on a HPLC (Shimadzu) equipped with Rezex ROA 300 x 7.8 mm column and UV-vis detector. A mobile phase of 0.005M H_2SO_4 was used. Ethyl acetate extract of the biocrude was analyzed on an Agilent GC-MS (7890 GC/5975C MSD) equipped with Agilent HP-5ms capillary column. Helium (99.999%, UHP grade) with column flow rate of 1.197 ml/min was used as carrier gas. The oven was programmed as follows: 40°C (8 min hold), ramped up (2°C/min) to 120°C (8 min hold), ramped up (5°C/min) to 220°C (no hold) and (20°C/min) to 250°C (no hold). The temperature of injector and detector was maintained at 300°C. The compounds were identified using National Institute of Standards and Technology (NIST) mass spectral library (2008, version 2.0f). The total organic carbon (TOC) content of the AC-treated HTL derived cotton biocrude was determined using a Sievers InnovOx Laboratory TOC analyzer (GE Instruments). Similar analyses were carried out with the samples of untreated.

2.1.6. Photocatalytic Reforming (PR) of Biocrude and Carboxylic Acids to H_2

Pt/TiO_2 photocatalyst (4.0 mg) was dispersed in 10 ml de-ionized water for 30 minute using ultrasonic bath and the dispersion was purged with N_2 for 30 min to displace oxygen. Lactic (LA), formic (FA), acetic (AA) and propionic (PA) acids were individually and in a mixed form dissolved in water to a final concentration of 50 mM. In another experiment LA, AA, FA PA were mixed in ratio of 3.65:1.80:1.27:1 to form biocrude acids stimulant. The reaction mixture (7 ml) was added to a quartz reactor and sealed with a butyl septum. The reactor headspace (4 ml) was purged with N_2. The headspace gas was sampled to confirm absence of O_2. The mixture was stirred by a magnetic needle and exposed to simulated solar irradiation obtained with 240 W Xe lamp and AM1.5G filter. The power density measured at the center of the reactor window was 100 mW/cm^2. During PR, headspace gas was withdrawn periodically and analyzed for H_2 on the Agilent 7890GC using the same column and method used for the analysis of product gas from HTL. Photreforming of AC-treated and untreated biocrude for H_2 generation was carried out using the same procedure as described earlier for individual acid and acid mixture. To achieve maximal reforming of the biocrude to H_2, the headspace was evacuated after 3 hour and purged with N_2 prior performing the next photoreforming cycle. The photoreforming cycles were continued until H_2 levels were below detection limit in GC analysis.

3. Results and Discussion

3.1. HTL of Cotton in the Presence of $NiSO_4$ Catalyst

Elemental analysis of cotton revealed that C, H, N and O were 45 wt%, 7.11 wt%, 0.2 wt% and 47.69 wt%, respectively. Figure 2a shows the product gas analysis from HTL of 1 gram cotton in the presence of 5 wt% $NiSO_4$ at 250°C and 650 psi. At "zero" reaction time, practically no H2 was observed, however, after 60 min of reaction 4.3 ml H_2 volume was detected. A total H_2 volume of 11.54 ml was observed after 120 min reaction time suggesting an almost linear increase in H_2 volume generation. The concentration of CH_4 in product gas was almost negligible at zero reaction time and did not change over the period of 2 hrs of reaction time. However, the volume of CO and CO_2 observed at zero reaction was about 25 ml. As the reaction progressed further, the volume of CO increased to 28 ml and remained constant.

Starting from zero reaction time to 2 hrs, the volumetric ratio of H_2: CO gaseous products increased from 0.0438 to 0.43 indicating 10 fold increase in H_2 over CO. Thus it appears that $NiSO_4$ has increased H_2 selectivity in the product gas phase. It is to be noted that in the absence of catalyst negligible quantities of H_2 were observed (data not shown). The CO_2 volume observed at zero reaction time (25 ml) was increased to 33 ml after 120 min reaction time. These results indicated 9.2%, 23% and 90% (volume basis) increase in CO, CO_2 and H_2, respectively over the period of 2 hrs reaction time at 250°C. The total product gas was estimated to be 10 wt% of the 1 gram cotton that was processed at 250°C for 2 hrs. After the HTL, the reactor contents were cooled to room temperature and centrifuged to recover the biocrude and residue. Based on the TOC analysis of the biocrude (1720 mg/L) and carbon content of cotton (estimated TOC 2811 mg/L), 61.2 wt% liquefaction of cotton was estimated (Figure 2b). The observed char residue was 28.8 wt%.
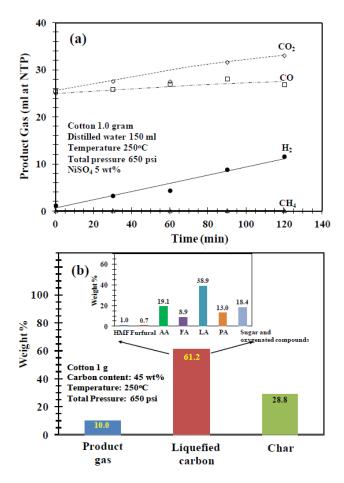
Figure 2. a) Product gas components observed during HTL of cotton at 250°C in the presence of $NiSO_4$ catalyst and b) mass balance showing liquefied carbon, total product gas, and char

3.2. Composition of the Cotton Biocrude

The liquefied cotton biocrude was analyzed by HPLC and GC-MS and the results obtained are presented in Table 1 and Table 2, respectively. HPLC analysis revealed presence of acetic, formic, lactic and propionic acids. Among these acids, lactic acid is the main component with the concentration of 1675 mg/L, whereas propionic acid was observed in minimum concentration of 459 mg/L. The total acids were estimated to be 79.88 wt% of cotton biocrude as per the following equation-

$$\% \; total \; acids = \frac{\sum \left(carbon \; content \; of \; C_1 \; to \; C_3 \; acids \; observed \right)}{total \; liquefied \; carbon \; in \; biocrude} \times 100$$

Table 1. HPLC Analysis of C_1-C_3 acids in the Cotton Biocrude Obtained after HTL at 250°C in presence of 5 wt% $NiSO_4$

C_1-C_3 acids, HMF, Furfural	Concentration (mgL^{-1})	
	Biocrude	AC-treated biocrude
Acetic acid	824	40.4
Formic acid	584	36.5
Lactic acid	1675	348.3
Propionic acid	459	39.6
HMF	30.7	------
Furfural	18.4	------

HMF and furfural were observed to be 1.69 wt% of liquefied biocrude. The remaining 18.4 wt% of biocrude was assigned to C_6 sugars (mainly glucose) and oxygenated hydrocarbons, which were thoroughly

analyzed by GC-MS using HP-5ms column and inbuilt NIST library. The complete mass balance of different compounds observed in liquefied cotton biocrude is shown in Figure 2b. The GC-MS analysis of the biocrude showing only major compounds (peak area >1% and confidence level >95%) is presented in Table 2. It indicates cyclic ketones and substituted cyclic ketones, quinone derivatives, phenols and substituted phenols, alcohols and acids. However, based on the mass balance analysis, it appears that the pathways leading to the formation of C_1-C_3 carboxylic acids dominated with the use of $NiSO_4$ catalyst and under the experimental conditions employed.

Table 2. Major compounds observed in the biocrude and AC-treated biocrude as analyzed by GCMS; >95% confidence level

Retention time (min)	Compounds observed	% peak area (biocrude)	% peak area (AC-treated biocrude)
6.25	2-Butanol, 3-methyl-, acetate	0.916	10.32
6.31	1H-Pyrazole, 1,5-dimethyl-	17.074	-----
6.60	2-Butenoic acid, ethyl	0.212	5.028
6.75	2-Pentanol, acetate	0.203	5.877
6.93	2-Butanone	1.482	-----
6.94	Hexanal, 2-ethyl-	-----	2.007
6.95	5,9-Dodecadien-2-one, 6,10-dimethyl-,(E,E))-	-----	1.772
8.16	2-Cyclopenten-1-one, 2-methyl	1.316	13.59
8.28	Acetic acid, 1-ethyl-2-methylpropyl ester	-----	1.080
8.67	Hexanoic acid, 2-propenyl ester	-----	2.297
8.80	2-Pentenoic acid	0.371	1.066
9.26	2(3H)-Furanone,dihydro-5-methyl	10.693	38.79
9.45	2-Furancarboxaldehyde, 5-methyl	1.353	-----
9.52	2-Cyclopenten-1-one,3-methyl	1.098	0.560
9.98	Formic acid, 2-propenyl ester	-----	3.459
9.99	2-Propen-1-ol	-----	3.680
10.11	Butanal, 2-methyl	1.011	-----
10.82	1,2-Cyclopentanedione, 3-methyl	5.893	3.124
11.54	Pentanoic acid, 4-oxo	0.757	1.387
12.48	2-Cyclopenten-1-one, 3-ethyl-2-hydroxy	1.396	-----
15.07	1H-Inden-1-one, 2,3-dihydro	2.467	-----
16.31	1,2,3-Benzenetriol	20.067	-----
17.54	Benzhydrazide, 3-nitro N2-(4-pyridylmethylene)-	1.889	-----
17.85	1,2,4-Benzenetriol	15.366	-----

3.3. Activated Charcoal (AC) Treatment of Biocrude

The cotton biocrude was treated with 10 mg/ml and 50 mg/ml activated charcoal and the visible difference in biocrude coloration is shown in inset of Figure 3. Activated charcoal at 10 mg/ml did not completely remove biocude color while colorless biocrude was obtained with 50 mg/ml activated charcoal treatment for 12 hours. Equal volumes (1 ml) of untreated biocrude and AC-treated samples were tested for photocatalytic H_2 generation using 0.4 mg/ml Pt/TiO_2 catalyst concentration.

The gas phase H_2 volume (ml at NTP) was estimated for 150 ml biocrude. As seen from Figure 3, PR of untreated biocrude did not generate any H_2 whereas 10 mg/ml and 50 mg/ml AC-treated biocrude generated 0.6 ml and 2.14 ml of H_2, respectively after 180 min.
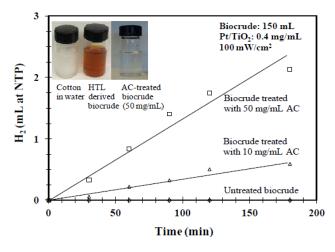

Figure 3. H_2 volume generated during PR of untreated cotton biocrude and biocrude treated with activated carbon at different concentrations

Although the colorless biocrude provided a six fold increase in H_2 volume generation, increasing AC concentration to 50 mg/ml contributed to loss of the C and H content of the biocrude. HPLC analysis of AC-treated cotton biocrude (Table 1) indicates significant removal of C_1-C_3 carboxylic acids as compared to the untreated biocrude. Alternate methods to selectively remove only the interfering compounds without affecting the carboxylic acids and sugars are currently under investigation. It can also be noticed from Table 2 that several oxygenated hydrocarbon compounds including the major ones such as 1H-pyrazole, 1,5-dimethyl-, 1,23-benzenetriol, 1,2,4 benzenetriol and 1,2 cyclopentanedione, 3-methyl have been removed by the AC treatment. It is to be noted that the AC has significant Ni ions adsorption capacity (97.8%) [18]; therefore, we inferred that negligible Ni ions were present during PR of AC-treated biocrude.

3.4. Photocatalysis of Biocrude Acid Component and AC-treated Biocrude

To further understand the role of the four major acid components of the biocrude towards the H_2 production, photoreforming of 50 mM LA, AA, FA and PA was carried out using procedure outlined in the Experimental section. Clearly, as seen from Figure 4 the acids differ in relative proficiencies as electron donors. Formic acid which is structurally simplest C_1 acid with one α hydrogen appears to be best electron donor producing maximum H_2 volume during 180 min reaction time. Under identical PR conditions, formic acid yielded 9.7 ml H_2 at NTP, which was 133 fold, 12.77 fold, and 2.95 fold higher than AA, PA and LA, respectively. LA, which is major acid in the biocrude, is also a better electron donor compared with the other two C_1-C_3 acids. On the other hand, acetic acid is relatively recalcitrant to photoreforming to H_2. LA, a C_3 acid differs from PA by the presence of a single hydroxyl group. The hydroxyl group in addition to the carboxyl group probably increases adsorption affinity of LA on the TiO_2 surface. This could facilitate better transfer of the photogenerated electrons to LA generating higher H_2

yields. A mixture containing 50 mM of FA, AA, PA and LA was also investigated for H_2 generation under identical PR conditions. Although the total H_2 content of this mixture was higher, the H_2 volume generated (6.65 mL) was about 1.5 fold lower than produced by the FA during PR, however, it was higher than LA, PA, and AA. This suggests that recalcitrant acids such as AA and PA in the acid biocrude probably reduce H_2 generation. This warrants further investigation of Pt/TiO_2 surface reactions of acid mixture during PR. In a separate experiment LA, PA, AA and FA were mixed in the concentration ratio found in the cotton biocrude. This acids mixture is referred to as 'biocrude acid simulant'. During 180 min of PR reaction, 1.16 mL H_2 was generated from the biocrude simulant. The biocrude stimulants were prepared with 0.1 and 10 fold acids concentrations to study the effect of concentration on H_2 evolution. The 0.1 fold biocrude stimulant generated significantly higher H_2 volume (4.13 mL), whereas 10-fold biocrude stimulant generated only 0.8 ml at NTP during PR. As the catalyst loading was held constant (0.4 mg/ml), higher number of active sites were available for the acid moieties present in 0.1 fold biocrude stimulant, which reflected into higher H_2 volume generation.
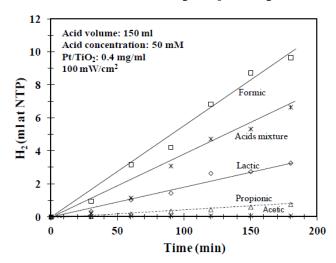

Figure 4. Comparative H_2 volume generated during PR of carboxylic acids and their mixture

It can be concluded that under the experimental conditions employed in this study, $NiSO_4$ catalyzed HTL process generates sufficient quantities of acids (~79 wt%) in the downstream biocrude. The biocrude can be used without dewatering or concentrating the acids for PR to enhance H_2 generation.

3.5. Combined Yields of H_2 from Integrated HTL and PR Processing of Cotton

To investigate total H_2 volume generation capacity of the biocrude simulant and actual biocrude during PR, multiple PR cycles were performed in the time interval of 180 min. After 180 min of PR reaction, the reactor headspace was evacuated by purging with N_2 until H_2 was undetectable in the GC analysis. The reactor was again exposed to simulated solar irradiation and next PR cycle was performed for 180 min. The H_2 volume generated from the biocrude acid simulant during four PR cycles is shown in Figure 5a. During PR cycle-1, cycle-2, cycle-3 and cycle-4, the maximum H_2 volume of 5.35 ml, 3.75ml, 1.98 ml, and 0.75 ml, respectively was observed after 180

min reaction time. The H_2 volume generated from the actual biocrude during four PR cycles is shown in Figure 5b. The maximum H_2 volume observed during PR cycle-1, cycle-2, cycle-3 and cycle-4 was 2.17 ml, 1.6 ml, 0.87 ml and 0.56 ml, respectively. These results indicate lower H_2 volume generation from the actual biocrude as compared with the biocrude acid simulant, which infers that the additional oxygenated compounds (Table 2) present in actual biocrude probably inhibited some of the H_2 generating reactions. The volumes of H_2 generated from each PR cycle were combined to obtain the total H_2 volume.
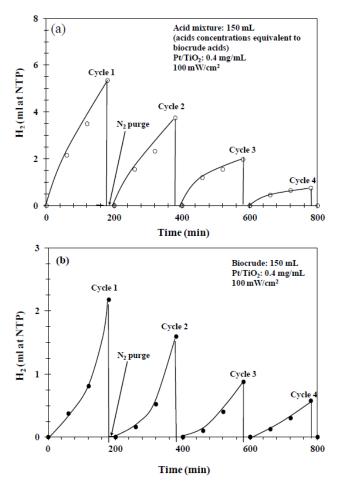

yields in terms of vol% are presented in Figure 6. It shows a total H_2 vol% produced from actual biocrude during four PR cycles was 17.82%. When H_2 vol% from PR and HTL is combined, a total of 20.93 vol% H_2 was extracted from cotton biocrude. This shows that by integrating HTL and PR processes, higher H_2 volume generation could be achieved. A maximum of 57.5 vol% H_2 was observed from biocrude acid simulant that contained only carboxylic acids during four PR cycles. This leads to the notion that the acids can be separated from the biocrude and treated with PR for higher H_2 volume generation.
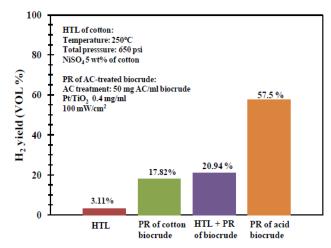

Figure 6. Total H_2 (vol%) extracted by integrating HTL of biomass and PR of HTL derived biocrude

4. Conclusions

HTL of cotton at 250°C in presence of $NiSO_4$ yielded 10 wt% product gas, 61.2 wt% liquefied biocrude and 28.8 wt% char. The product gas phase during HTL was found to contain 3.12 vol% H_2 whereas the PR of biocrude performed during cycles 1 to 4 amounts to a total of 5.22 ml. When the H_2 volume generated from HTL was combined with the total H_2 volume produced during four PR cycles, a total of 20.94 vol% was extracted from the biocrude. Thus by integrating HTL and PR, higher H_2 volume generation could be achieved.

Acknowledgement

Figure 5. a: H_2 volume generated during PR of C_1-C_3 acids mixture, and b) AC-treated cotton biocrude

The H_2 yield (vol%) was determined as per the following equation-

$$H_2 \; yield = \frac{\sum \left(H_2 \; volume \; generated \; in \; each \; cycle \right)}{\left(\begin{array}{c} total \; theoretical \; H_2 \; volume \\ of \; all \; acids \; present \; in \; mixture \end{array} \right)} \times 100$$

The total H_2 volume of acids mixture was estimated based on the theoretical H_2 content of all acids and their concentrations used to prepare the acids mixture. For biocrude, the H_2 yield was determined as the ratio of total H_2 volume generated in all PR cycles and H_2 volume content of 150 ml AC-treated biocrude. The total H_2 volume for the AC-treated biocrude was estimated based on the acids concentration reported in Table 1. These acids were present in the biocrude after AC treatment. The H_2

References

[1] Lewis, N., "Powering the Planet", *MRS Bulletin*, 32 (10). 808- 820. 2007.

[2] Rittmann, S., and Herwig, C., "A comprehensive and quantitative review of dark fermentative biohydrogen production", *Microbial Cell Factories*, 11 (1.). 115-133. 2012.

[3] Wang, D., Czernik, S., Montane, D., Mann, M., and Chornet, E., "Biomass to hydrogen via fast pyrolysis and catalytic steam reforming of the pyrolysis oils or its fractions", *Industiral & Engineering Chemistry Research*, 36 (5). 1507-1518. 1997.

[4] Elliot, D.C., Neuenschwander, G.G., Hart, T.R., Butner, R.S., Zacher, A.H., Engelhard, M.H., Young, J.S., and McCready, D.E.,

"Chemical processing in high-pressure aqueous environments. 7. Process development for catalytic gasification of wet biomass feedstocks", *Industiral & Engineering Chemistry Research*, 43 (9). 1999-2004. 2004.

[5] Tungal, R., and Shende, R.V., "Subcritical aqueous phase reforming of wastepaper for biocrude and H_2 generation", *Energy & Fuels*, 27 (6). 3194-3203. 2013.

[6] Tungal, R., and Shende, R.V., "Hydrothermal liquefaction of pinewood (Pinus ponderosa) for H_2, biocrude and bio-oil generation", *Applied Energy*, 134. 401-412. 2014.

[7] Kondarides, D.L., Daskalaki, V.M., Patsoura, A., and Verykios X.E., "Hydrogen production by photo-induced reforming of biomass components and derivatives at ambient conditions", Catalysis Letters, 122. 26-32. 2008.

[8] Fu, X., Long, J., Wang, Z., Leung, D.Y.C., Ding, Z., Wu, L., Zhang, Z., Li, Z., and Fu, X., "Photocatalytic reforming of biomass: A systematic study of hydrogen evolution from glucose solution", *International Journal of Hydrogen Energy*, 33 (22), 6484-6491. 2008.

[9] Tungal, R., Shende, R.V., and Christopher, L., "Nickel catalyzed high pressure hydrothermal processing of biomass for H_2 production", *Journal of Energy Power Engineering*, 5. 504-514. 2011.

[10] Li Y, Lu G, Li S. Photocatalytic production of hydrogen in single component and mixture systems of electron donors and monitoring adsorption of donors by in situ infrared spectroscopy. Chemosphere. 2003 Aug; 52(5):843-50.

[11] Lanese, V., Spasiano, D., Marotta, R., Sommar, I.D., Lisi, L., Cimio, S., Andreozzi, R., 2013. Hydrogen production by photoreforming of formic acid in aqueous copper/TiO_2 suspensions under UV-simulated solar radiation at room temperature, Int. J. Hydrogen Energy, 23, 9644-9654.

[12] Heciak,A, Morawski, A Grzmil, B, Mozia, S August–September 2013; Cu modified TiO_2 photocatalysts for decomposition of acetic acid with simultaneous formation of C_1–C_3 hydrocarbons and hydrogen Applied Catalysis B: Environmental; Volumes 140–141,108-114.

[13] Maraschi, Daniele Dondi, Andrea Serra, Antonella Profumo, Armando Buttafava, Angelo Albini Swine sewage as sacrificial biomass for photocatalytic hydrogen gas production: Explorative study Andrea Speltini, Michela Sturini, Federica International journal of hydrogen energy 39 (2014) 11433 e11440.

[14] Ela Ero glua, ˙Inci Ero glua, Ufuk Gündüzb, Lemi Türkerc, Meral Yücelb Biological hydrogen production from olive mill wastewater with two-stage processes International Journal of Hydrogen Energy 31 (2006) 1527-153.

[15] Mohan, S.V., and Karthikeyan, J., "Removal of lignin and tannin colour from aqueous solution by adsorption onto activated charcoal", *Environment Pollution*, 97 (1-2). 183-187. 1997.

[16] Mudoga, H.L., Yucel, H., and Kincal, N.S., "Decolorization of sugar syrups using commercial and sugar beet pulp based activated carbons", *Bioresource Technology*, 99 (9). 3528-3533. 2008.

[17] Orozco, R.L., Redwood, M.D., Leeke, G.A., Bahari, A., Santos, R.C.D., and Macaskie, L.E., "Hydrothermal hydrolysis of starch with CO_2 and detoxification of the hydrolysates with activated carbon for bio-hydrogen fermentation", *International Journal of Hydrogen Energy*, 37 (8). 6545-6555. 2012.

[18] Hashimoto, K., Irie, H., and Fujishima, A., "TiO_2 photocatalysis: a historical overview and future prospects", *Japanese Journal of Applied Physics*, 44 (12). 8269-8285. 2005.

[19] Hussein, A.M., and Shende, R.V., "Enhanced hydrogen generation using ZrO_2-modified coupled ZnO/TiO_2 nanocomposites in the absence of noble metal co-catalyst", *International Journal of Hydrogen Energy*, 39 (11). 5557-5568. 2014.

[20] Ni, M., Leung, M.K.H., Leung, D.Y.C., and Sumathy, K., "A review and recent developments in photocatalytic water-splitting using TiO_2 for hydrogen production", *Renewable & Sustainable Energy Reviews*, 11. 401-425. 2007.

[21] Rossetti, I., "Hydrogen production by photoreforming of renewable substrates", *ISRN Chemical Engineering*. 1-21. 2012.

[22] Hasar, H., "Adsorption of nickel (II) ions from aqueous solution onto activated carbon prepared from almond husk", *Journal of Hazardous Materials*, 97 (1-3). 49-57. 2003.

[23] Yin, S., Tan, Z., 2012. Hydrothermal liquefaction of cellulose to bio-oil under acidic, neutral and alkaline conditions, Applied Energy, 92 (C), 234-239.